Spatio-Temporal Diversity in Ultra-Wideband Radio

J.M. Cramer, *Member, IEEE**, R.A. Scholtz, *Fellow, IEEE**, M.Z. Win, *Senior Member, IEEE*†
*Communication Sciences Institute, EEB 500
Department of Electrical Engineering - Systems
University of Southern California, Los Angeles, CA 90089-2565 USA
†Wireless Systems Research Department
Newman Springs Laboratory, AT&T Labs-Research
Rm 4-147, 100 Schulz Dr., Red Bank, NJ 07701-7033 USA

Abstract— **One of the potential benefits of the UWB radio is its multipath resolution. The implications are multipath components which might not be resolved as distinct arrivals in more narrowband systems, may be separately identified in UWB systems. This paper explores some of the propagation characteristics associated with UWB signals, based on measured data.**

I. Introduction

POTENTIAL applications for ultra-wideband (UWB) systems include those where wireless communication in dense multipath environments is required. These are environments where the fine-time resolution and reduced signal level fluctuations of received UWB signals may prove to be advantages over more narrowband communication waveforms [3],[8],[9]. Given the available multipath resolution, it is of interest understand the gains available through the use of diversity techniques. A temporal characterization of diversity in the UWB propagation channel has been accomplished through the use of rake receivers [10],[2]. The work reported here initiates the development of channel models which incorporate the angle-of-arrival as well as the time-of-arrival of the multipath signal components in the UWB propagation channel.

This paper begins with a discussion on channel statistics, using measured indoor UWB propagation data. The first and second moments of the temporal and angular power distributions for several indoor UWB channels are calculated. Next, under a definition of diversity as the ability to overcome transient blockages in the signal paths, an attempt is made to determine the angle at which the received signal components were transmitted, based upon the received angle, the known line-of-sight (LOS) path length and the propagation distance of the signal component.

II. Propagation experiment

For the purpose of characterizing the indoor UWB propagation channel, a channel sounding experiment was conducted in an office building. Briefly, a transmitter was placed at a fixed location in an office building, while a receiver was moved to a number of different points. At each location, 49 sets of data were collected on a 7×7 planar grid of sensors with 6-inch inter-sensor spacing.

The floor plan is shown in Figure 1 with rays drawn to indicate the LOS path from the transmitter to the receiver for the four sets of received data that will be discussed below. Concentric circles at one meter increments in the radius are shown as an overlay. Further details of the measurement experiment can be found in [10].

A delay-and-sum beamformer was applied to the measured array of data, followed by a processing algorithm defined in [1] as Sensor-CLEAN, generating information on the time-of-arrival (TOA) and angle-of-arrival (AOA) of the multipath components. As in [1], γ was selected as 0.10 for the results presented here. The time resolution of these results is determined by the sampling rate of 20.48 Gsamples/second at which the measurements were taken. The beamformer output was calculated for each available time sample, at one degree increments in azimuth angle. The angular resolution of the techniques employed here, or minimum separation in angle at which coincident pulses can be identified as distinct, is limited by the dimension of the measurement array aperture to approximately 16°.

III. Indoor UWB Channel Statistics

A. Definitions

In order to characterize the indoor UWB channel, the definition of several quantities is required. First define the SNR of a received UWB signal as

$$SNR = 10 \log \frac{\sum_{n=0}^{N-1} s^2(n,\theta)}{\sigma^2} \quad dB \tag{1}$$

where $s(n,\theta)$ is the beamformer output corresponding to the largest incident signal, normalized by the number of contributing sensors, N is the number of time samples where the signal is assumed to be nonzero, θ is the angle-of-arrival and σ^2 is the variance of the noise floor. According to this definition, $n = 0$ then corresponds to the leading edge of the incident signal. For the results presented here, a UWB channel will be defined by the SNR of the LOS

This work was supported in part by the Army Research Office under the ASSERT Program Grant No. DAA955-97-1-0245. and in part by TRW Space and Electronics Group.

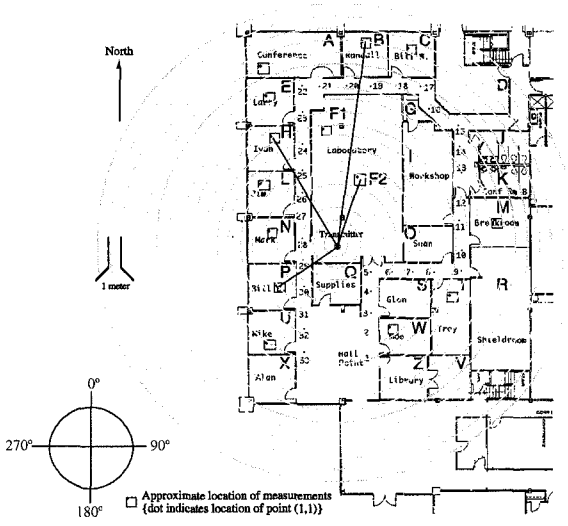

Fig. 1. Floor plan of building with rays indicating LOS paths

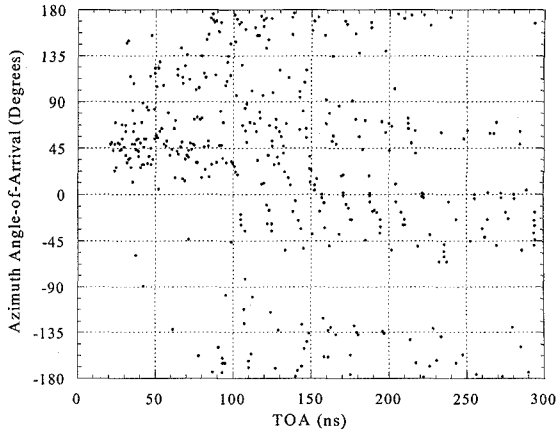

Fig. 2. Recovered signal AOA and TOA information for location P

path. Typical parameters by which the temporal and spatial distribution of signal energy is characterized include the first moment and the root of the second moment of the power delay profile. Assuming discrete time signals these moments are defined for the received signal on the kth sensor, $r(n,k)$, as [5]

$$\overline{T}_k = \frac{\sum_{n=0}^{N-1} nr^2(n,k)}{\sum_{n=0}^{N-1} r^2(n,k)} \quad (2)$$

$$\sigma_{T,k} = \sqrt{\frac{\sum_{n=0}^{N-1} \left(n-\overline{T}_k\right)^2 r^2(n,k)}{\sum_{n=0}^{N-1} r^2(n,k)}} \quad (3)$$

The delay spread is often reported as the median of a collection of measurements [5]. The spatial distribution of the signal energy can be measured by the first and root second moments of the received angular profile, [4],

$$\overline{\phi} = \frac{\sum_{k=0}^{K-1} \phi_k \beta_k^2}{\sum_{k=0}^{K-1} \beta_k^2} \quad (4)$$

$$\sigma_\phi = \sqrt{\frac{\sum_{k=0}^{K-1} \left(\phi_k-\overline{\phi}\right)^2 \beta_k^2}{\sum_{k=0}^{K-1} \beta_k^2}} \quad (5)$$

where β_k is the amplitude of the signal component incident from angle k. Equation (4) is referred to as the power-weighted average AOA, and equation (5) is called the RMS AOA. Note that the angular spread must be defined over some measurement window in time, and β_k^2 then can be interpreted as the energy accumulated at angle k during the time window.

B. Application to measured data

Considering the measurement from the transmitter to location P in the floor plan, a scatter diagram of the arrival locations in time and angle is shown in Figure 2. Here, the LOS path is incident at an azimuth angle of 49^o and a time of 20.8 ns, followed immediately by multipath components. The distance between the transmitter and the center of the receiver array can be approximated from the arrival time of the LOS path and a separate measurement taken at a known 1 meter separation between the transmitter and receiver. This then takes into account any delays in the circuitry or the cables. Using this technique, the distance between the transmitter and the center of the receiver array in room P is determined to be approximately 5.47 meters. The signal-to-noise ratio can be determined according to equation (1) as 27.4 dB. These measurements can be seen to correlate well with the floor plan. For the signal arrivals in Figure 2, the median RMS delay spread, $\sigma_{T,med}$, where the median is taken over the 49 sets of data in the array, is 50.1 ns. The median value of the average delay spread, calculated over the 49 sets of data, is $\overline{T}_{k,med}$= 64.8 ns. In [6], median RMS delay spread values between 25 and 50 ns were reported for narrowband propagation measurements in an office building at 1.5 GHz. The angular spread is calculated as a single value for the entire time window. This does not provide any indication of variations in this quantity as a function of time. For this case, the average angular spread is calculated to be $\overline{\phi}$=71.6^{o}and the RMS angular spread is σ_ϕ=66.7^o. Note that these quantities are weighted by the amplitude of the incident signal, which is not shown in the scatter diagram.

The next measurement is for data received at location $F2$, approximately 5.61 meters from the transmitter. The SNR for this case was determined to be 34.3 dB. The scatter diagram for the detected arrivals is shown in Figure 3. As mentioned above, the transmitter and receiver were located in the same room with a steel pole between them, just to the left of the LOS path. The LOS path is incident upon the geometric center of the array at 21.3 ns after the start of the data collection, from an azimuth angle of -157^o. As can be seen from the figure, this pole tends to shadow the array from arrivals in a number of directions. The median RMS delay spread for this channel is calculated as $\sigma_{T,med}$=44.9 ns, comparable to the measurements made at location P.

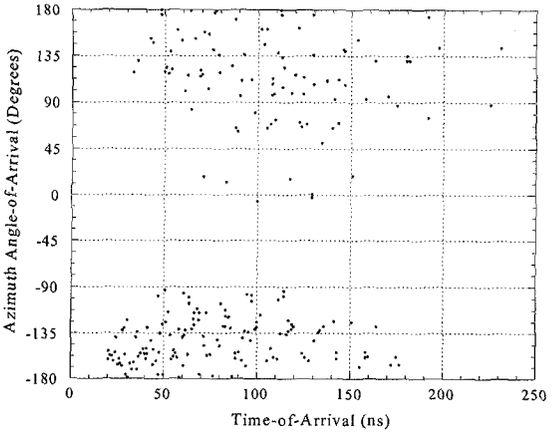

Fig. 3. Recovered signal AOA and TOA information for location $F2$.

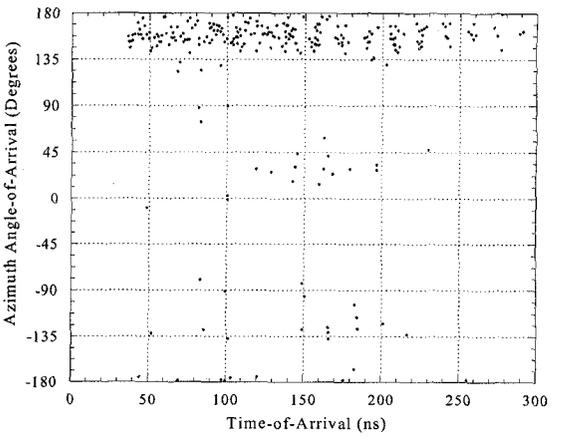

Fig. 4. Recovered signal AOA and TOA information for measurement at location H

The median of the average delay spread is $\overline{T}_{k,med}$=58.6 ns. Note that the difference in $\overline{T}_{k,med}$ between this set of measurements and the previous set, where the LOS path lengths are similar, indicates that a larger percentage of the received signal energy is concentrated in the earlier arrival times. Considering the angular statistics, the average azimuth power-weighted angle-of-arrival is $\overline{\phi}$=-162.1^o, which is close to the azimuth angle at which the LOS path arrives. The RMS angular spread is σ_ϕ =30.9^o, a much smaller value than that obtained in the previous case.

The next set of data was measured at location H in the floor plan, and corresponds to a SNR of 21.5 dB. The transmitter and receiver are separated by approximately 10.21 meters, including several walls. The largest signal component impinges on the array at 40.6 ns after the start of data collection, from an azimuth angle of 159^o. The scatter diagram corresponding to this scenario is shown in Figure 4. Here, the median RMS delay spread is 52.6 ns, while $\overline{T}_{k,med}$ is equal to 95.5 ns. As far as the angular information, the average azimuth AOA is given by $\overline{\phi}$=157.8^{o}and the RMS angular spread is σ_ϕ=20.8^o. Once again, $\overline{\phi}$ is close to the angle at which the largest signal component arrives, and σ_ϕ is actually smaller that in either of the two cases above, perhaps due to the longer propagation distance and the receiver therefore being situated further away from some set of scatterers.

The final case considered here corresponds to a much lower SNR of 7.9 dB. For this set of measurements, the receiver was located at position B, a distance of 16.9 meters from the transmitter, with several walls separating them. The delay spread numbers are calculated as $\overline{T}_{k,med}$=126.4 ns and $\sigma_{T,med}$=73.9 ns. The larger value of $\overline{T}_{k,med}$ can be attributed in large part to the distance between the transmitter and the receiver, while the increase in $\sigma_{T,med}$ can be explained by the lack of a dominant LOS signal component, resulting in a more uniform spread of the received signal energy as a function of time. In terms of the angular characteristics, $\overline{\phi}$=-165.1^o, and the RMS angular spread is σ_ϕ =30.2^o.

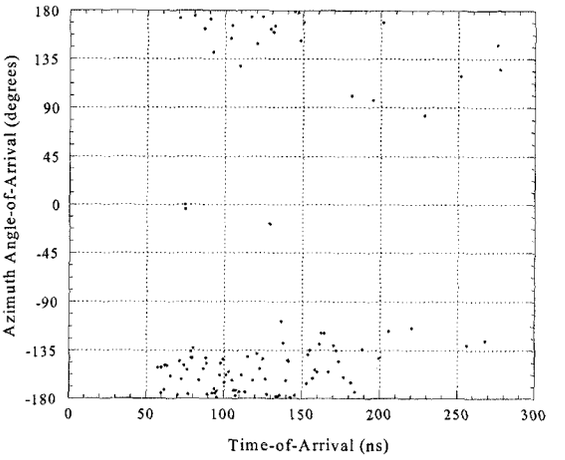

Fig. 5. Recovered signal AOA and TOA information for measurement at location B

Table 1 summarizes the temporal and angular information presented above. From this table and the discussion above, it is seen that although there appears to be a rough correlation between the parameters and the SNR or propagation distance, the strongest dependence is on the geometry of the situation. This is similar to the narrowband case [4] and makes the properties difficult to predict without taking into account the floor plans.

SNR (dB)	$\overline{T}_{k,med}$ (ns)	$\sigma_{T,med}$ (ns)	$\overline{\phi}$ $(^o)$	σ_ϕ $(^o)$
27.4	64.8	50.1	71.6	66.7
34.3	58.6	44.9	-162.1	30.9
21.5	95.5	52.6	157.8	20.8
7.9	126.4	73.9	-165.1	30.2

Table 1. Summary of propagation statistics

C. Distribution Functions

A goal of this research is to develop statistical measures against which radio algorithms can be tested. As a prelimi-

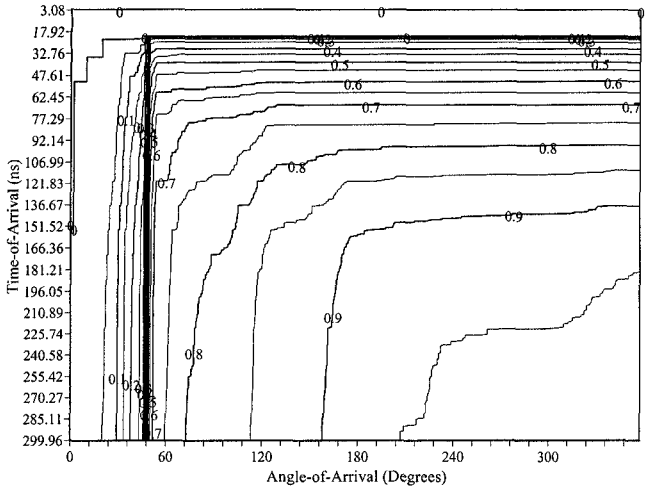

Fig. 6. CDF for energy arrival in room P

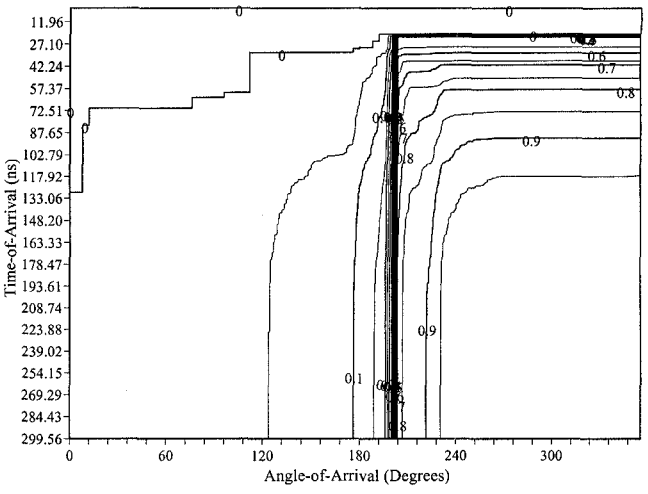

Fig. 7. CDF for energy arrival at $F2$

nary result, the cumulative distribution function (CDF) for the arrival of signal energy is calculated from the multipath arrival information. For an angular increment of $\Delta\theta$ and a sampling frequency of $\frac{1}{\Delta t}$ seconds, this CDF is calculated according to

$$F\left(\theta = k\Delta\theta, t = n\Delta t\right) = \frac{1}{E}\sum_{j=0}^{k}\sum_{m=0}^{n}\beta\left(m,j\right) \qquad (6)$$

where $k = 0, ..., K-1$, $n = 0, ..., N-1$, β is the amplitude of the component found at time m and angle j, and E is the value resulting from allowing the summations to run over all time samples and angles. An assumption is made here that the energy in the received waveform does not vary as a function of the arrival time or angle. Figure 6, Figure 7, Figure 8 and 9 show the CDF for the arrival of signal energy for each of the four cases considered above, respectively. As above, it appears that the geometry of the situation has a stronger affect on the shape of the function than does other parameters such as distance from the transmitter to the receiver.

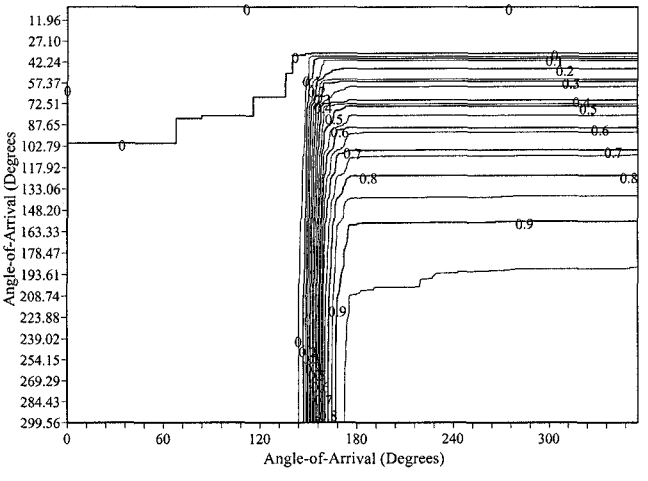

Fig. 8. CDF for energy arrival in room H

IV. Implications for Diversity

Considering the applications for UWB radio mentioned above, it is of interest to examine diversity algorithms for these systems. In particular, for the indoor environment, a useful performance measure is the ability of UWB communication systems to overcome transient blockages in the received signal paths, through the coherent addition of multipath signal components in a rake-type receiver. Given this measure, the resources required to maintain communications with a certain probability can be calculated.

Consider the transmitter and receiver pair shown in Figure 10, where the ellipse describes all paths of identical propagation length corresponding to a single reflection. Let θ_T represent the angle at which a signal component emanates from the transmitter, and let θ_R represent the received angle. Given θ_R, the signal propagation distance and the LOS propagation distance, the angle θ_T at

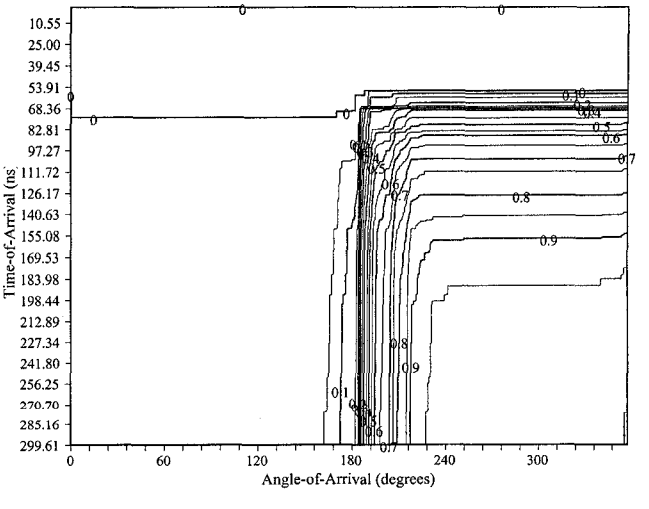

Fig. 9. CDF for energy arrival in room B

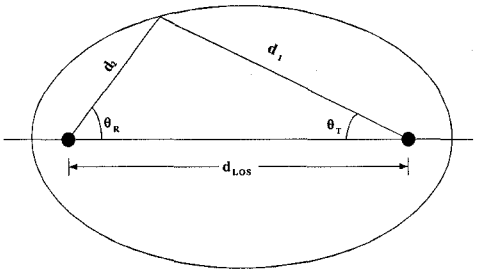

Fig. 10. Ellipse which describes signal reflection

which the component emanates from the transmitter can be uniquely determined, based on the assumption of a single reflection. In general, the greater the angular spread of distinct paths between the transmitter and the receiver, the greater the probability of overcoming a transient blockage in the signal path, or equivalently, the lower the probability that all paths are not available. Denote the LOS propagation distance by d_{LOS}, and the total propagation distance of the signal by $d = d_1 + d_2$. The eccentricity of the ellipse is then given by $e = d_{LOS}/d$. Defining

$$l = 0.5\left(d - \frac{d_{LOS}^2}{d}\right) \tag{7}$$

the distance d_2 can be calculated according to,

$$d_2 = \frac{l}{1 - e\cos(\theta_R)} \tag{8}$$

The angle θ_T is then given by,

$$\theta_T = \cos^{-1}\left(\frac{d_{LOS} - d_2\cos\theta_R}{d - d_2}\right) \tag{9}$$

where this angle must be reflected about the major axis of the ellipse if θ_R is negative.

In practice, the utility of this approach is limited by the lack of an analytic technique for discriminating signal components arriving at the receiver after a single reflection from those corresponding to multiple reflections. At present, correlating the calculated locations of the reflectors against the floor plan given above seems to be the best technique. Also, it remains to include elevation angle in the descriptions offered above. For the first set of data above, the location of the reflections determined by this technique are shown in Figure 11. The transmitter is located at the origin of the coordinate system, and the calculated location of the reflections are indicated throughout the building.

V. Conclusions

In this paper, measures describing propagation in the indoor UWB channel were given for several different channels in order to characterize typical results. More channels must be considered in order to generate any statistically significant conclusions. Ultimately, it is of interest to assess the performance of spatial diversity algorithms in the indoor UWB propagation channel, in particular, to calculate the probability of overcoming transient blockages through the use of multiple signal paths.

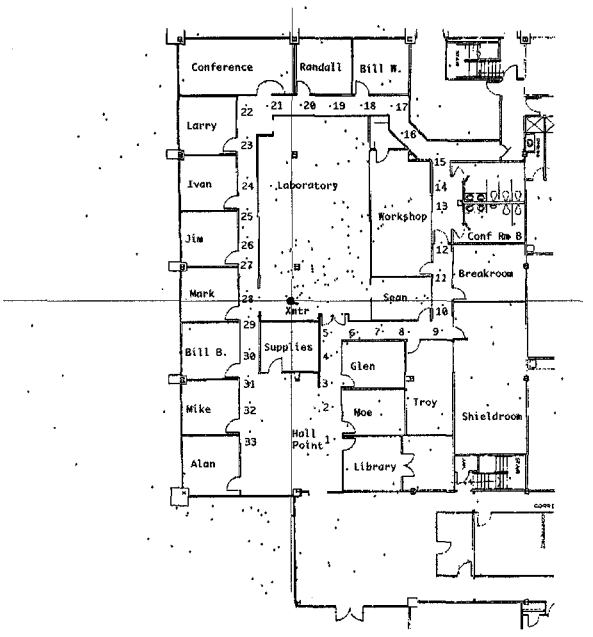

Fig. 11. Calculated locations of signal reflections, overlayed on the floor plan

The authors wish to acknowledge Time Domain Corporation for their assistance in collecting the UWB propagation data utilized in this paper.

References

[1] R. J.-M. Cramer, R.A. Scholtz, M.Z. Win, "On the analysis of UWB communication channels", to be published in *Proc. of Milcom '99.*

[2] R. J.-M. Cramer, M.Z. Win and R.A. Scholtz, "Impulse Radio Multipath Characteristics and Diversity Reception", *Proc. of ICC '98*, vol. 3, p. 1650-1654.

[3] S.S. Kolenchery, J.K. Townsend, J.A. Freebersyser, "A Novel Impulse Radio Network for Tactical Military Wireless Communications", Proc. of Milcom '98.

[4] J. Litva and T. K-Y. Lo, *Digital Beamforming in Wireless Communications*, Artech House Publishers, 1996.

[5] D. Parsons, *The Mobile Radio Propagation Channel*, Halsted Press, 1992.

[6] A.A.M. Saleh and R.A. Valenzuela, "A statistical model for indoor multipath propagation", *IEEE JSAC*, vol. 5, no. 2, pp. 128-137, 1987.

[7] R.A. Scholtz, "Multiple Access with Time-Hopping Impulse Modulation," in *Proc. Milcom*, Oct. 1993.

[8] R.A. Scholtz and M.Z. Win, "Impulse Radio", *Personal Indoor Mobile Radio Conference*, Helsinki, Finland, Sept. 1997, Printed in *Wireless Communications: TDMA vs. CDMA*, S.G. Glisic and P.A. Leppänen, eds., Kluwer Academic Publishers, 1997.

[9] M.Z. Win and R.A. Scholtz, "Comparisons of analog and digital impulse radio for multiple-access communications," in *Proc. IEEE Int. Conf. on Comm.*, pp. 91–95, June 1997. Montréal, Canada.

[10] M.Z. Win, R.A. Scholtz, and M.A. Barnes, "Ultra-wide bandwidth signal propagation for indoor wireless communications," in *Proc. IEEE Int. Conf. on Comm.*, pp. 56–60, June 1997. Montréal, Canada.